DOE/PC/70027-8

Hydrodynamics of Fischer-Tropsch Synthesis in Slurry Bubble Column Reactors

Quarterly Technical Progress Report

for the Period 1 June 1986 - 31 August 1986

Dragomir B. Bukur, James G. Daly, John Swank, S. A. Patel and Garry B. Tatterson*

Texas A&M University

Department of Chemical Engineering

College Station, Texas 77843

September 1986

Prepared for United States Department of Energy Under Contract No. DE-AC22-84PC70027

*Dr. G. B. Tatterson is with the Department of Mechanical Engineering

NOTICE

PATENT STATUS

TECHNICAL STATUS

TABLE OF CONTENTS

I. Abstract

Experiments were conducted in Unit AM-2G (5.1 cm ID, 305 cm tall glass bubble column) at 265°C using FT-300 paraffin wax as the liquid medium and nitrogen as the gas. During these experiments, movies representative of the flow field were taken as well as data for the dynamic gas disengagement (DGD) technique.

An improved photographic technique was employed to obtain pictures, for bubble size analysis, in experiments conducted in the Unit AM-9G (22.9 cm ID, 300 cm tall glass bubble column). During these experiments, measurements of the average gas hold-up were made at temperatures of 200°C and 265°C using FT-300 paraffin wax as the liquid medium and nitrogen as the gas.

Dynamic gas disengagement data collected in this quarter in the Unit AM-2G were analyzed to obtain results indicating bubble sizes, volume fraction distributions and Sauter mean diameters. Results are interpreted in terms of a bimodal distribution for velocities greater than 1 cm/s and a unimodal distribution for a velocity of 1 cm/s. Analysis of the dynamic gas disengagement data collected in the previous quater in the Unit AM-9G was extended to include Sauter mean diameters.

Photographs of bubbles taken in the previous quarter, in the Unit AM-2G, were analyzed by image processing to obtain cummulative bubble size distributions and Sauter mean diameters.

A viewing port was installed in the Unit AM-9S (24.1 cm ID, 300 cm tall stainless steel column) for the purpose of obtaining photographs of bubbles near the center of the column.

II. Objective and Scope of Work

The overall objective of this contract is to determine effects of reactor geometry, distributor design, operating conditions (i.e., temperature and gas flow rate), and oxygenated compounds on hydrodynamics of slurry bubble column reactors for Fischer-Tropsch synthesis, using a hard paraffin wax as the liquid medium. To accomplish these objectives, the following specific tasks will be undertaken.

Task 1 - Project Work Plan

The objective of this task is to establish a detailed project work plan covering the entire period of performance of the contract, including estimated costs and manhours expended by month for each task.

Task 2 - Bubble Column Reactor Design/Construction

Two bubble columns made of borosilicate glass of approximately 2" ID and 9" ID, and 10 ft tall will be designed and assembled for measurement of the gas hold-up and the bubble size distribution. After the design, procurement of equipment and instrumentation, and construction of the unit is completed, a shakedown of test facilities will be made to verify achievement of planned operating conditions. During this period instruments will be calibrated.

Task 3 - Process Variable Studies

The objective of this task is to determine the effect of various system variables (e.g. gas flow rate, temperature, and addition of minor amounts of oxygenated compounds) on hydrodynamic properties using the two bubble columns (2" and 9" ID) and different types of distributors. All experiments will be conducted using nitrogen at atmospheric pressure. It

is planned to determine the following hydrodynamic characteristics: gas hold-up, flow regime characterization, bubble size distribution, and the gas-liquid interfacial area.

Task 4 - Correlation Development and Data Reduction

Correlations based on our experimental data for prediction of average gas hold-up and the gas-liquid interfacial area will be developed.

III. Summary of Progress

Results for the Sauter mean diameter and bubble size distribution were obtained by DGD and photography in conjunction with image analysis. Results were obtained in the Units AM-2G and AM-9G (DGD only).

The results obtained in the Unit AM-2G (T = 265°C, 1.85 mm single hole orifice) and the Unit AM-9G (T = 265°C, 19 x 1.85 mm PP) indicate that the column diameter does not have a significant effect on the Sauter mean diameter. In Runs 6-1 (AM-2G) and 1-3 (AM-9G) where the hold-up values were similar, the value of d_{vs} was approximately 0.5 mm in the "foamy" regime and 1.0 mm in the "non-foamy" regime for both columns. An additional run in the Unit AM-9G (1-4) produced lower hold-ups. The Sauter mean diameter for this run was slightly larger (1.2 mm) in the "non-foamy" regime.

Results obtained by the photographic method in the Unit AM-2G (1.85 mm single hole orifice plate distributor) for d_{vs} indicate that the Sauter mean diameter remains fairly constant (approximately 1.8 mm) regardless of operating conditions or flow regime. This is different than that observed by DGD, where d_{vs} is lower in the "foamy" regime. This difference is probably due to the fact that in the photographic method, a finite number of bubbles are counted and presence of a few large bubbles distorts results; whereas, all the bubbles are taken into account by the DGD technique.

The effect of distributor type (1.85 mm orifice plate distributor and the 40 μm SMP) on d_{vs} was also determined by the photographic technique. The Sauter mean diameters obtained with the SMP distributor are approxi-

mately 0.5 mm in the "foamy" regime and 0.2 mm in the "non-foamy" regime, which is significantly smaller than that obtained for the 1.85 mm orifice plate distributor by the same method.

IV. Detailed Description of Technical Progress

A. Task 1 - Project Work Plan

The work on this Task was completed during the first quarter of the project.

B. Task 2 - Bubble Column Reactor Design/Construction

The work on this task was completed during the fourth quarter of the project.

C. Task 3 - Process Variable Studies

3.1 Experiments in the Unit AM-2G

Additional experiments were performed in the 5.1 cm ID, 305 cm tall bubble column (Unit AM-2G) with FT-300 wax as the liquid medium at 265°C for velocities of 1 cm/s to 12 cm/s. A 1.85 mm single hole orifice plate distributor and a SMP with an average pore size of approximately 40 μm were employed in the experiments. The experiments were performed with the following objectives: 1) to take movies of the flow field at various velocities for future presentations, and 2) to obtain data from dynamic gas disengagement method.

Movie pictures were taken with a 16 mm Bolex movie camera equipped with an automatic lens. The movies were shot at 24 frames per second using 400 ASA Kodak film. Lighting was supplied by a single 750 W bulb located behind the column approximately six inches below the field of view.

Gas hold-up values as well as movie pictures were obtained in Run 7-1 (1.85 mm distributor) and Run 7-2 (40 μm SMP) for gas velocities of 1 cm/s to 12 cm/s (increasing order). The gas hold-up results obtained in both runs were similar to those previously obtained.

In Run 6-1 (1.85 mm distributor), velocities of 1 to 12 cm/s (in-

creasing order) at a temperature of 265°C were employed in order to obtain average gas hold-ups and DGD data.

3.2 Experiments in the Unit AM-9G

Experiments were made in the 22.9 cm ID, 300 cm tall glass column (Unit AM-9G) with two perforated plate (PP) distributors having 19 holes of 1.85 mm or 1 mm in diameter for velocities ranging from 1 cm/s to 12 cm/s. Experiments were conducted at a temperature of 265°C with the 19 x 1.85 PP using both an increasing and a decreasing order of gas velocities. Experiments with the 19 x 1 mm PP were performed using an increasing order of gas velocities at temperatures of 200°C and 265°C. For all experiments, a minimum time of one and a half hours per velocity was allowed for $u_g \leq 5$ cm/s (measurements every 30 min.) and one hour per velocity (measurements every 20 min.) for $u_g > 5$ cm/s. The primary purpose of the experiments was to obtain photographs for image analysis.

Various lighting arrangements and lenses were tried in the Unit AM-9G in order to obtain better quality photographs for bubble size and bubble size distribution analysis. Two different arrangements were used, one for low gas velocities ($u_g \leq 5$ cm/s) and one for gas velocities greater than 5 cm/s. A Cannon, AE1/P (35 mm SLR) camera and a Vivitar Model 283 flash were used for all photos. The flash was mounted approximately 25 cm from the column at a 45° angle from the front of the column. At low gas velocities, a Cannon 135 mm lens mounted on a Cannon Auto Bellows with an extension of 110 mm was employed. At the higher gas velocities, a 50 mm Cannon lens was mounted on the Cannon Auto Bellows with a 70 mm extenison. Photographs were taken during all experiments following the second gas

hold-up measurement for all velocities (u_g = 1 - 12 cm/s) at heights of 40, 110, and 200 cm.

The average gas hold-ups obtained during these experiments agree with those previously reported.

3.3 Modication of the Unit AM-9S

A viewing port, for the purpose of obtaining photographs of bubbles near the center of the column, was constructed and installed in the Unit AM-9S (305 cm tall, 24.1 cm ID) at a height of 120 cm. Figure 1 shows a sketch of the viewing port. The viewing port was checked for leaks with water, and the column was pressure checked to 20 psig.

D. Task 4 - Correlation Development and Data Reduction

4.1 Sauter Mean Diameter by Dynamic Gas Disengagement Method

The development of the equations needed for using the dynamic gas disengagement (DGD) technique and the procedure for obtaining ϵ_{goi}, $u_{B,i}$, f_i, and $d_{B,i}$ were presented in the previous Quarterly Report (March - May, 1986) and will not be repeated here. Analysis of the results obtained from the DGD technique has been extended to include the determination of the Sauter mean diameter, d_{vs}.

The results obtained for ϵ_{goi} and $d_{B,i}$ may be used to obtain the Sauter mean diameter. The overall or average gas hold-up may be expressed as:

$$\epsilon_{go} = V_g/V_T \qquad (1)$$

where V_g is the volume of gas in the gas-liquid dispersion and V_T is the expanded volume. This equation can be rewritten as:

$$\epsilon_{go} = \Sigma N_i V_i/V_T \qquad (2)$$

where N_i is the number of bubbles of size i and V_i is the volume associated

with bubbles of size i.

Therefore, the hold-up associated with a bubble of size i can be expressed as:

$$\epsilon_{goi} = N_i V_i / V_T \tag{3}$$

or

$$N_i = \epsilon_{goi} V_T / V_i \tag{4}$$

The volume associated with bubbles of size i is given by:

$$V_i = \pi d_{B,i}^3 / 6 \tag{5}$$

and the total volume is:

$$V_T = \pi D^2 L_o / 4 \tag{6}$$

Substituting equations (5) and (6) into equation (4) yields:

$$N_i = 3\epsilon_{goi} D^2 L_o / 2 d_{B,i}^3 \tag{7}$$

which may be used to calculate the number of bubbles of size i.

By definition, the Sauter mean diameter, d_{vs}, is:

$$d_{vs} = \Sigma N_i d_{B,i}^3 / \Sigma N_i d_{B,i}^2 \tag{8}$$

Substituting equation (7) into (8), yields upon rearrangement:

$$d_{vs} = \frac{\Sigma \epsilon_{goi}}{\Sigma \epsilon_{goi} / d_{B,i}} \tag{9}$$

4.1.1 Discussion of Results

Figure 2 (Unit AM-2G, Run 6-1, T = 265°C, u_g = 1 - 12 cm/s, 1.85 m single hole orifice plate) shows the normalized change in the liquid level as a function of time for velocities of 1, 3, 5, and 9 cm/s. For a velocity of 1 cm/s, there is a unimodal distribution, which is depicted by the single line. For velocities of 3, 5, and 9 cm/s two lines appear giving rise to a bimodal distribution. The second line associated with u_g = 3

cm/s has a different slope than that of the same lines associated with u_g = 5 cm/s and 9 cm/s. This is attributed to the fact that foam was present at 3 cm/s, but not at 5 cm/s or 9 cm/s.

Figure 3 shows the effect of superfical gas velocity and flow regime on the bubble size. The size of the small bubbles produced in Run 6-1 remains essentially constant ranging from 0.35 mm to 0.45 mm for all velocites studied regardless of the flow regime (i.e. "foamy" or "non-foamy"). The large bubbles tend to be slightly larger in the "foamy" regime (u_g = 2, 3, and 4 cm/s). However, once the foam is broken ($u_g \geq 5$ cm/s), the size of the large bubbles remains constant at approximately 2.6 cm.

The volume fraction of bubbles of size i (i = small and large), for various gas velocities is shown in Table 1. In the "foamy" regime ($2 \leq u_g \leq 4$ cm/s), about 80% to 86% of the gas hold-up was due to the small bubbles produced. Once the foam was broken (u_g = 5 cm/s), the volume fraction of small bubbles decreased to 50%. For velocities ranging from 5 cm/s to 12 cm/s, there is a gradual decrease in the fraction of small bubbles accompanied by increase in fraction of large bubbles.

These trends support our visual observations. When foam is present, there is a large amount of small bubbles present. Once the foam breaks, the number of small bubbles decreases which can be seen by the drop in the volume fraction of small bubbles from 80% to 50%. As the velocity increases, the rate at which slugs are produced also increases, giving rise to an increase in the volume fraction of large bubbles.

Comparison of d_{vs} obtained in AM-9G and AM-2G

Run 1-3 (increasing order of gas velocities) and Run 1-4 (decreasing

order of gas velocities) were performed in Unit AM-9G; whereas, Run 6-1 (increasing order of gas velocities) was performed in Unit AM-2G. All three runs were conducted at 265°C using FT-300 wax as the liquid medium. The runs performed in the Unit AM-9G employed the 19 x 1.85 mm PP distributors, and the run in the Unit AM-2G employed the 1.85 mm single hole orifice plate distributor.

The average gas hold-up values obtained in Run 1-3 and Run 6-1 were essentially the same. Foam was produced in both runs and broke at u_g = 5 cm/s. In Run 1-4 (unit AM-9G, decreasing order of velocities), the gas hold-up values obtained in the "non-foamy" regime ($u_g \geq 5$ cm/s) were slightly lower than those produced in Runs 1-3 and 6-1. Also, in Run 1-4, foam was never produced (i.e. "non-foamy" flow regime for all velocities).

The effect of column diameter, flow regime, and gas velocity on the Sauter mean diameter is shown in Figure 4. The Sauter mean diameter is not affected by the column diameter. In Run 6-1 (unit AM-2G) and Run 1-3 (Unit AM-9G), in which the hold-up values were essentially the same for all velocities, the Sauter mean diameters are also essentially the same. In Run 1-4 (unit AM-9G), in the "non-foamy" regime ($u_g \geq 5$ cm/s), values for the Sauter mean diameter are slightly higher than in Runs 1-3 and 6-1. This is expected since the average gas hold-ups obtained in Run 1-4 were slightly lower than in Runs 1-3 and 6-1 (i.e. lower hold-up-larger bubbles).

In Runs 1-3 and 6-1 foam was produced at velocities ranging from 2 cm/s to 4 cm/s. The values for d_{vs} in this regime ("foamy") are substantially lower than in the "non-foamy" regime, $u_g \geq 5$ cm/s (i.e. "foamy" -

$d_{vs} \cong 0.5$ mm; "non-foamy" - $d_{vs} \cong 1.0$ mm), which is as expected.

4.2 Bubble Size Distribution by Image Process Analysis

Photographs of the flow field in the AM-2G glass column and AM-9G glass column obtained during the past two quarters were catalogued and selected photos were enlarged for bubble size distribution determination by image processing analysis. Photographs obtained from both columns have been analyzed using an image analyzer, but only the results from the AM-2G glass column have been evaluated and are presented in this report.

4.2.1 Image Analysis Technique for Bubble Size Determination

Photographs selected for analysis are enlarged to 8" by 10" and analyzed on a Zeiss image analyzer located in the Biology department at the University of Texas in Austin. An illustration of the image analysis system is shown in Fig. 5. The TV camera (1) takes a picture of the enlarged photograph and displays the photograph on the TV screen (2). The image is also stored in IBAS II (3), the array processor. The image analyzer is only able to distinguish between shades of gray; therefore, when bubbles overlap, the image analyzer treats the bubbles as a single image. Due to this problem, photographs cannot be analyzed automatically. The IBAS II software package allows the user to select only those bubbles which are clear and distinct and remove all other images from the screen. The selection of bubbles is performed by tracing over the bubbles one wants to analyze (using the digitizer tablet with mouse (4)). Once this is complete, a variety of object specific parameters can be calculated and displayed on the data monitor (5) and/or printer (6). The parameters are stored, for further analysis, on an 8" floppy disk located in IBAS I (7). The parameters which are most useful for characterization of the bubble

size and bubble size distribution are the average diameter (arithmetic average of the minimum and maximum length of the elongated bubble) and the diameter of the area equivalent circle.

The IBAS II system is exited once the data associated with the object specific parameters has been stored on the floppy disk. Next, the software package, for obtaining statistical data, associated with IBAS I, is implemented. This package calculates the variance, geometric and arithmetic means, and the second and third moments associated with the object specific parameters (i.e. average diameter and diameter of area equivalent circle). Once these values have been printed out on the printer, the classification software package is loaded and classification results are obtained. The classification results include frequency and cummulative frequency distributions of the object specific parameters based on classes of bubbles (i.e. bubbles are divided into 40 groups). In general, approximately 500 bubbles were analyzed per photograph.

4.2.2 Discussion of Results

Results illustrating the effect of distributor design, operating procedure (temperature and gas velocity), and column height on d_{vs} and the bubble size distribution were obtained for experiments conducted in the Unit AM-2G. Experiments were made at temperatures of 200°C and 265°C for gas velocities of 1 cm/s to 12 cm/s. The liquid medium used was either pure FT-300 wax or FT-300 with the addition of oxygenates (5 wt% stearyl alcohol (SA) or 5 wt% SA + 5 wt% stearic acid). The distributors employed in the study were the 1.85 mm single hole orifice plate distributor and SMP with an average pore size of 40 μm.

4.2.2.1 1.85 mm Single Hole Orifice Plate Distributor

Photograph selection was made from the data in Run 4-1 (T = 265°C, u_g = 1 cm/s - 12 cm/s, FT-300) as the base case. Photos selected from the subsequent runs (i.e. different operating conditions) were limited.

Effect of Column Height

The effect of column height on the bubble diameter and the cummulative bubble size distribution for Run 4-1 are shown in Figures 6 and 7, respectively. In general, the bubble diameter remains fairly constant in the lower to middle section of the column (40 cm to 120 cm), and then decreases towards the top of the column (180 cm) (Figure 6) regardless of the flow regime (u_g = 3 cm/s - "foamy", u_g = 1 or 9 cm/s "non-foamy"). The same trend was also observed for a limited number of velocities studied in the other runs. The cummulative bubble size distribution (Figure 7) supports the results associated with the bubble mean diameter. Figure 7 shows the cummulative bubble distribution for a velocity of 3 cm/s at heights of 40 cm, 120 cm, and 180 cm. The cummulative distribution associated with heights of 40 cm and 120 cm are essentially the same, while the shift to the left in cummulative distribution at a height of 180 cm indicates a decrease in the bubble size. The same trend was also observed at other velocities in Run 4-1 as well as in the other runs.

Effect of Operating Procedure

The effect of operating procedure in the "foamy" and "non-foamy" regime on the cummulative bubble size distribution at a height of 120 cm is shown in Figures 8 and 9, respectively. A comparison between the bubble size distribution in the "foamy" and "non-foamy" regime is shown in Figure

8. In Runs 4-1, 4-4, and 4-5, foam was produced at 3 cm/s. In Runs 4-2 and 4-3, there was not any foam present at 3 cm/s. As can be seen in Figure 8, there is a greater number of small bubbles present in Runs 4-1, 4-4 and 4-5, as opposed to Runs 4-2 and 4-3. Figure 9 shows that the bubble size distribution is the same regardless of operating procedure, provided gas hold-ups are similar, and one operates in the "non-foamy" regime. In Run 4-5, (10% oxygenates), the gas hold-up was slightly higher at a velocity of 9 cm/s than in Runs 4-1, 4-2, and 4-3. This is reflected in the fact that the bubble distribution is shifted to the left for Run 4-5 (i.e. higher concentration of smaller bubbles).

The effect of velocity on the Sauter mean diameter is shown in Figure 10. In general, the Sauter diameter appears to remain fairly constant (1.8 mm) regardless of temperature (200°C or 265°C) and gas velocity (u_g = 1 cm/s to 9 cm/s) when pure FT-300 wax is used (Runs 4-1, 4-2, and 4-3). The addition of oxygenates (Runs 4-4 and 4-5) causes a decrease in the value of the Sauter mean diameter (~1 mm for $u_g \geq 3$ cm/s). This can be partially explained by the fact that in the runs with oxygenated compounds, slightly higher hold-ups were obtained than in runs without oxygenates at these velocities. This increase in the gas hold-up is associated with an increase in the number of small bubbles produced. From our visual observations, the concentration of small bubbles is higher near the wall of the column. Since the photographic technique employed is only able to photograph bubbles near the wall, it is possible this may have caused this trend.

The effect of large bubbles and the number of bubbles one counts on the Sauter mean diameter is discussed in Section 4.3.

4.2.2.2 40 μm SMP Distributor

For the experiments conducted with the SMP distributor, only photographs at 120 cm were analyzed when foam was present. Therefore, the effect of column height on the Sauter mean diameter or bubble size distribution can not be determined from the data analyzed.

Effect of Operating Conditions

The effect of operating conditions on the Sauter mean diameter and the bubble size distribution is shown in Figures 11 and 12, respectively. The Sauter diameter remains fairly constant regardless of the velocity, temperature, or liquid medium provided the flow regime (i.e "foamy" or "non-foamy") is the same (See Figure 11). In the "foamy" regime, the Sauter diameter is approximately 0.5 mm and in the "non-foamy" regime approximately 0.2 mm. The same trend exists for the bubble size distribution as seen in Figure 12. In Figure 12 (u_g = 7 cm/s), there is a shift towards the left in the curves associated with Runs 5-2 and 5-3 ("non-foamy"). This indicates that smaller bubbles are present in the "non-foamy" regime.

Smaller bubbles were observed with the 1.85 mm distributor in the "foamy" regime, whereas, larger bubbles were observed in the "foamy" regime with the SMP relative to bubbles in the "non-foamy" regime. The difference in trends can be explained by the fact that foam tends to be comprised of larger bubbles than those in the liquid (except slugs). In the experiments with the SMP, when foam was present, it filled the entire column (ϵ_g = 70%), therefore, the photographs taken were photographs of the foam. Whereas, in experiments conducted with the 1.85 mm orifice, foam does not

fill the entire column; hence, photographs taken are of the bubbles in the gas-liquid dispersion near the wall of the column.

4.3 Drawbacks to the Photographic Method for Determining the Sauter Mean Diameter

There are limitations and drawbacks to the photographic technique for determining the Sauter mean diameter. The photographic technique only allows for the analysis of bubbles near the wall of the column which may not be representative of the bubbles in the entire column.

Once photographs of bubbles have been taken, the bubble sizes associated with the bubbles in the picture need to be determined by either a mechanical method or by image process analysis. Regardless of the method employed, the bubble sizes obtained will be biased toward larger bubbles. The prejudice toward larger bubbles arises from the fact that in general, most of the large bubbles will be sized in a photograph (clearly defined and in focus); whereas, not all the small bubbles will be sized (too many and alot are out of focus). Due to the finite number of bubbles which are counted the Sauter mean diameter will be significantly affected by the large bubbles. This is evident in the following examples.

Given a bimodal distribution with 500 bubbles of 0.5 mm in diameter and 1 bubble 10 mm in diameter, the Sauter mean diameter is 4.7 mm. However, given 500 bubbles of 1 mm in diameter and 1 bubble 10 mm in diameter, the Sauter mean diameter is 2.5 mm. This result is contrary to what one would expect. The results obtained from the image analysis procedure show that tiny bubbles ($d_B < 0.5$ mm) are present; therefore, by counting only a relatively small number of these tiny bubbles the values for the Sauter mean diameter will be larger than they actually are.

4.4 Comparison of d_{vs} Obtained from the DGD and Photographic Techniques.

The Sauter mean diameter was determined by the DGD technique and the photographic technique in the Unit AM-2G with the 1.85 mm single hole orifice plate distributor.

The results obtained by DGD showed a difference in the value of d_{vs} between the "foamy" and the "non-foamy" regime. In the "foamy" regime (2 cm/s $\leq$ u_g $\leq$ 4 cm/s), the Sauter mean diameter was approximately 0.5 mm; whereas, in the "non-foamy" regime ($u_g \geq 5$ cm/s), the Sauter mean diameter is larger (~1 mm). In the "non-foamy" regime, it increases slightly with increases in the gas velocity.

The Sauter mean diameter determined from the photographic technique did not show discernible trends with the gas velocity. The value for d_{vs} obtained from the photographic technique was approximately 1.8 mm for all velocities.

The differences in results for d_{vs} obtained by the two different methods can be explained by the fact that the DGD technique takes in to account all the bubbles in the column, whereas, the photographic technique only takes into account the bubbles near the wall. Also, only a limited number (ca. 500) of these bubbles are counted. To get more accurate results by the photographic method one would need to size much greater number of bubbles (ca. 5000) and to obtain photographs of the flow field inside the column. However, this would be a rather lengthy and costly procedure.

V. Future Work

The following activities are planned for the next quarter.

(a) Obtain photographs of the flow field near the center of the column in the Unit AM-9S.

(b) Perform experiments in the Unit AM-2G using reactor waxes supplied by Mobil and UOP.

(c) Continue the analysis of data for bubble size distribution.

VI. Nomenclature

$d_{B,i}$	bubble diameter corresponding to bubbles of size i (cm)
d_{vs}	Sauter mean diameter (cm)
D	column diameter (cm)
f_i	fraction of bubbles of size i
L_o	expanded height (cm)
N_i	number of bubbles of size i
T	column temperature (°C)
V_g	volume of gas in the gas-liquid dispersion (cm^3)
V_i	volume of bubble of size i (cm^3)
V_T	total volume (liquid and gas) (cm^3)
$u_{B,i}$	bubble rise velocity corresponding to bubbles of size i (cm/s)
u_g	superficial gas velocity (cm/s)

Greek Letters

ϵ_{go}	average gas hold-up (fraction)
ϵ_{goi}	gas hold-up corresponding to bubbles of size i (fraction).

Acronyms

DGD	dynamic gas disengagement
DOE	Department of Energy
ID	inside diameter
PP	perforated plate
SMP	sintered metal plate
TAMU	Texas A&M University

Subscripts

L	large bubbles
S	small bubbles

Table 1. Hydrodynamic parameters obtained from dynamic gas disengagement method (Unit AM-2G, Run 6-1)

u_g (cm/s)	ϵ_{go} (%)	$u_{B,S}$ (cm/s)	$u_{B,L}$ (cm/s)	$d_{B,S}$ (cm)	$d_{B,L}$ (cm)	f_S (-)	f_L (-)
1	4.0	19.6	–	NA	–	1.0	–
2	15.4	4.2	39.3	.044	3.1	.81	.19
3	22.5	3.5	41.2	.040	3.4	.86	.14
4	27.3	2.2	41.8	.035	3.5	.82	.18
5	17.5	3.5	36.2	.040	2.6	.47	.53
7	22.0	3.3	36.1	.037	2.6	.51	.49
9	24.4	2.8	36.2	.037	2.6	.39	.61
12	26.4	3.6	39.0	.040	3.0	.31	.69

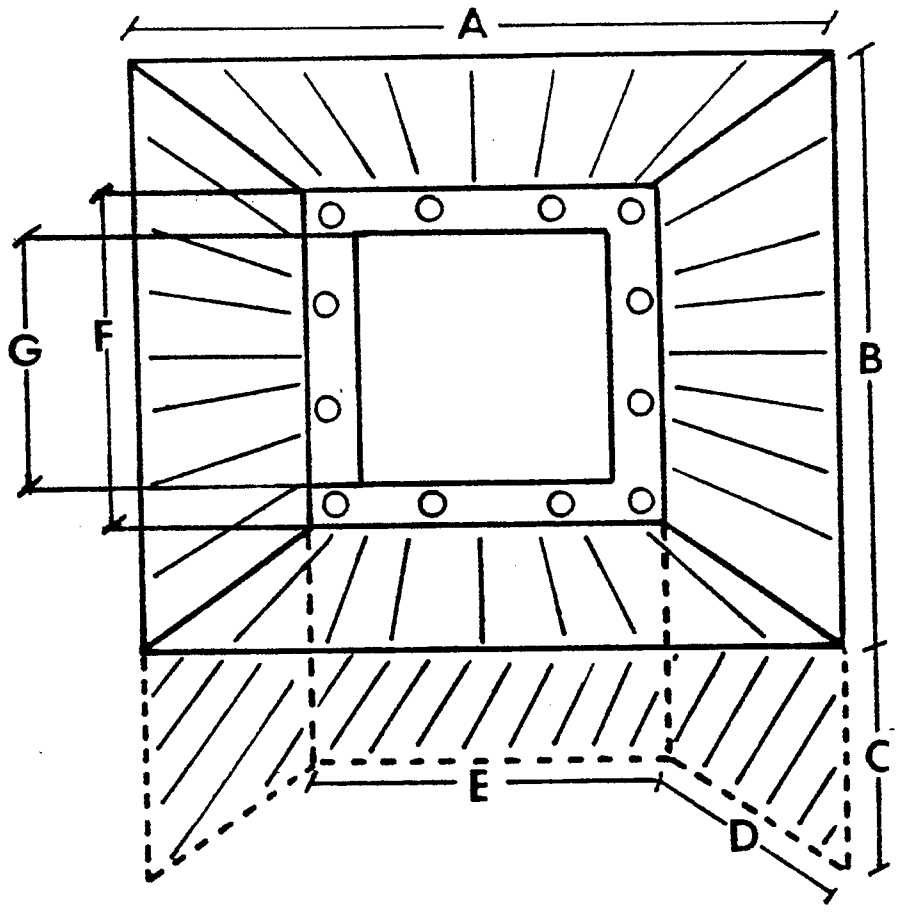

A = 20 cm ; B = 20 cm ; C = 5 cm ; D = 10.5 cm
E = 10 cm ; F = 10 cm ; G = 7.6 cm

Figure 1. Viewing port for Unit AM-9S

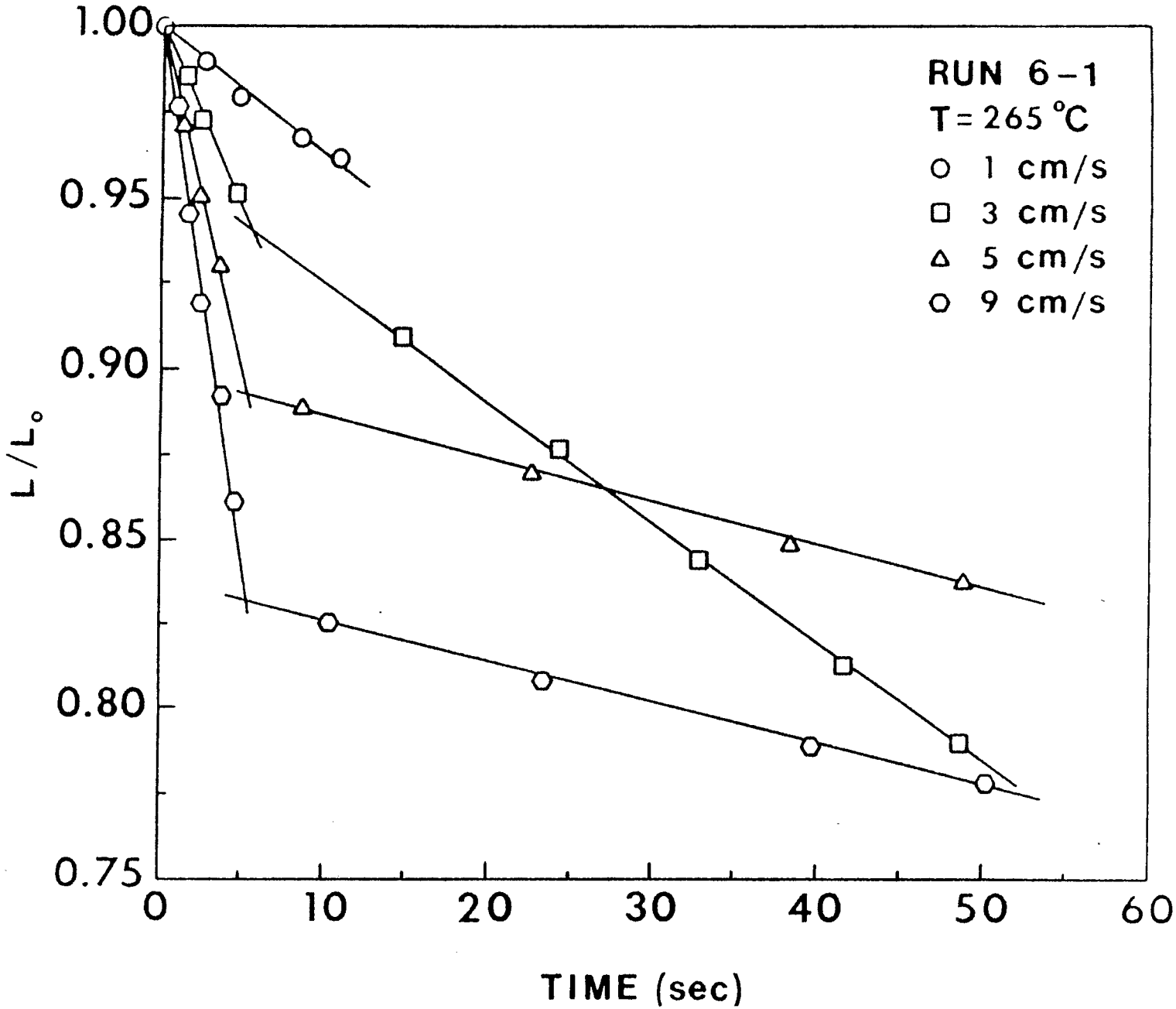

Figure 2. Change in the normalized liquid level as a function of time and velocity (Unit AM-2G; 1.85 mm single hole orifice plate distributor; DGD method)

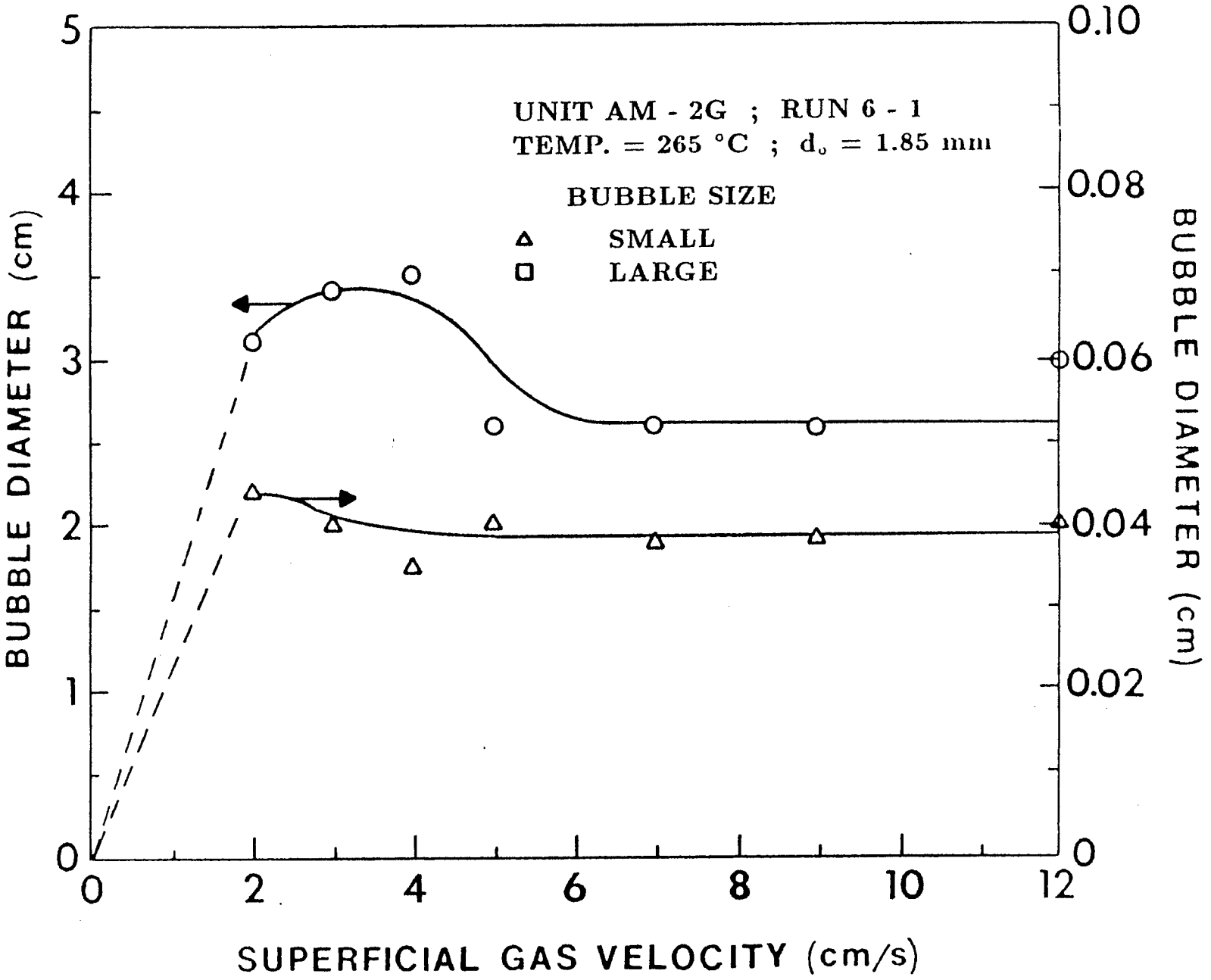

Figure 3. Effect of superficial gas velocity on bubble size (DGD method)

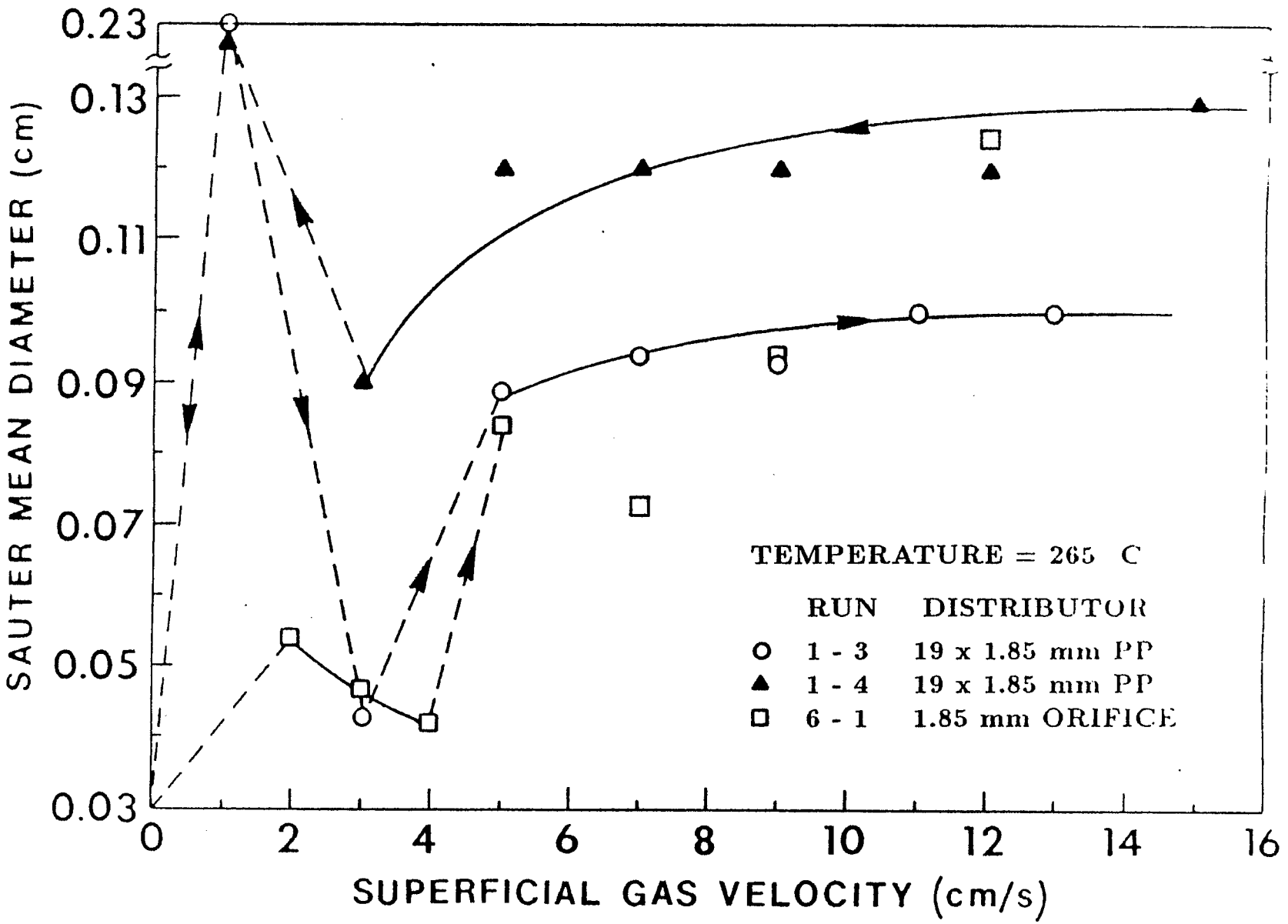

Figure 4. Effect of start-up procedure, column diameter, and superficial gas velocity on the Sauter mean diameter (open symbols - increasing gas velocities; solid symbols - decreasing gas velocities; DGD method)

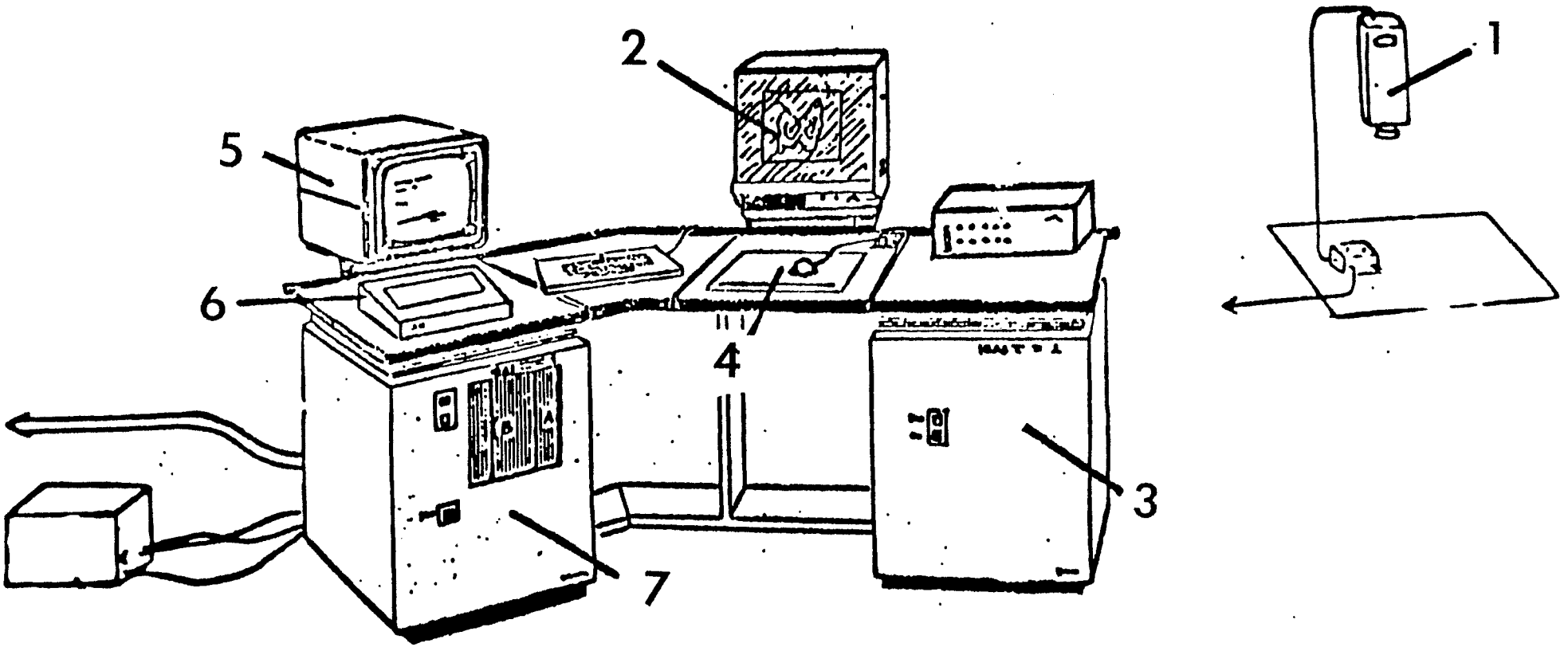

Figure 5. Image process analysis system

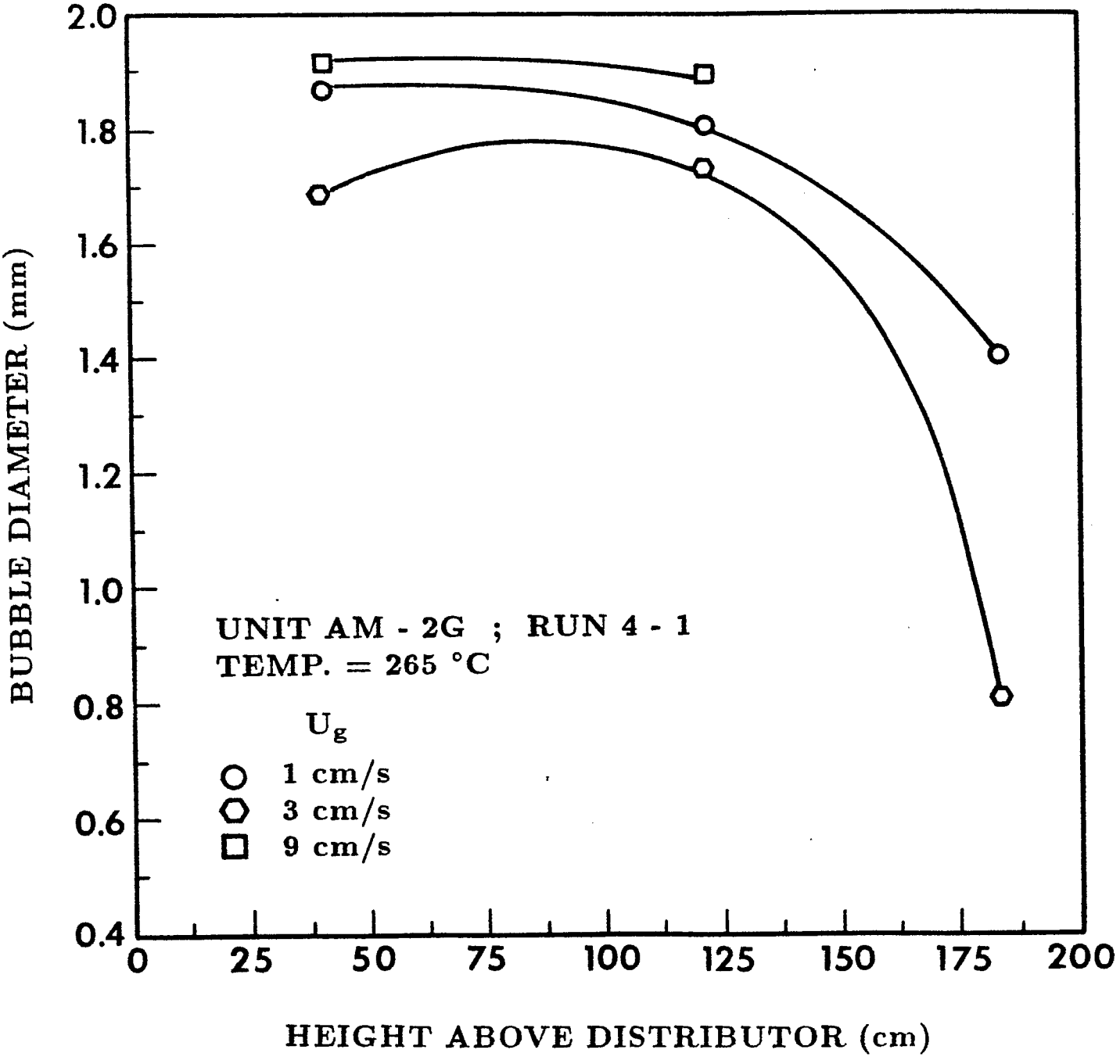

Figure 6. Effect of height above the distributor on the bubble size (by photography)

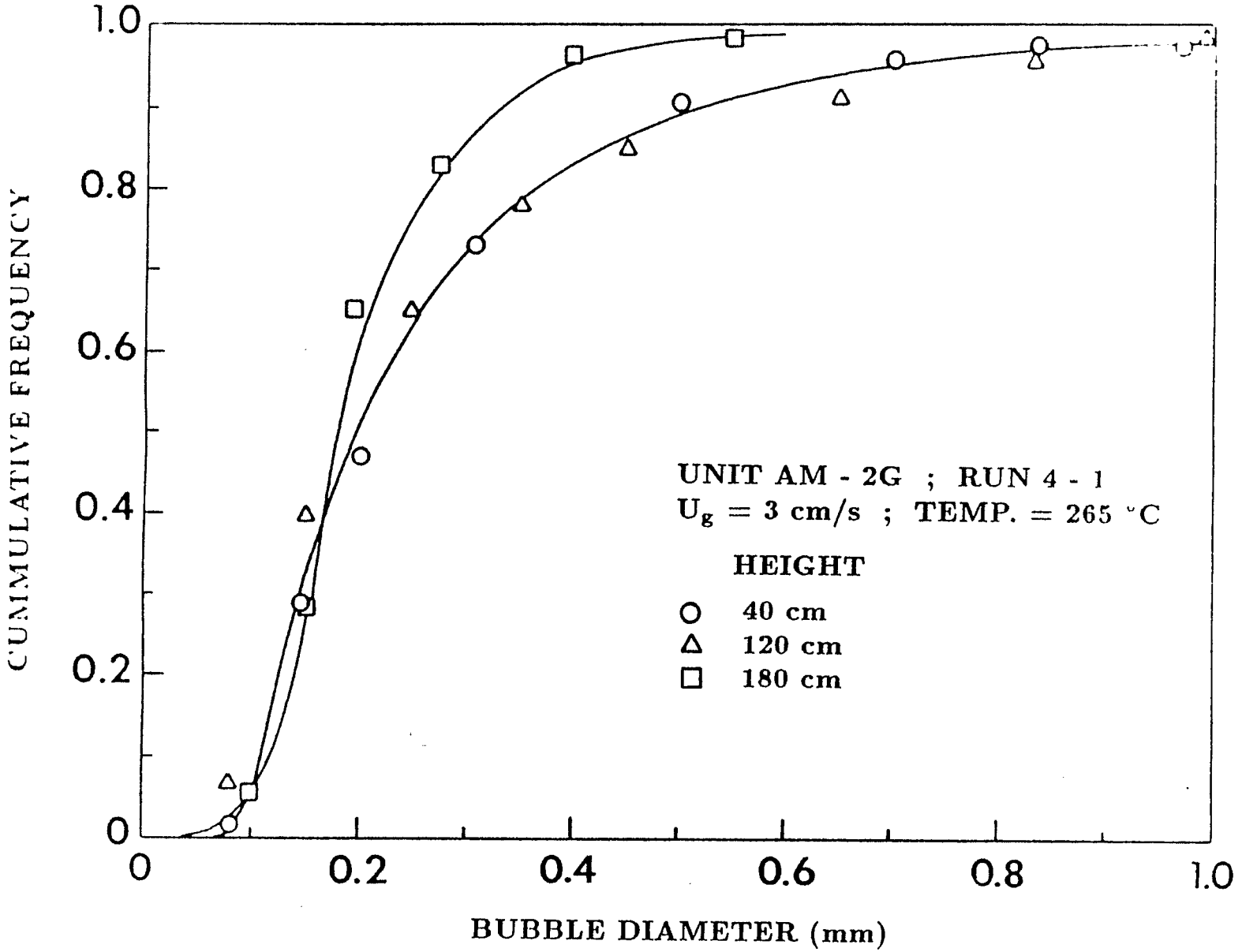

Figure 7. Effect of height above the distributor on the bubble size distribution (by photography)

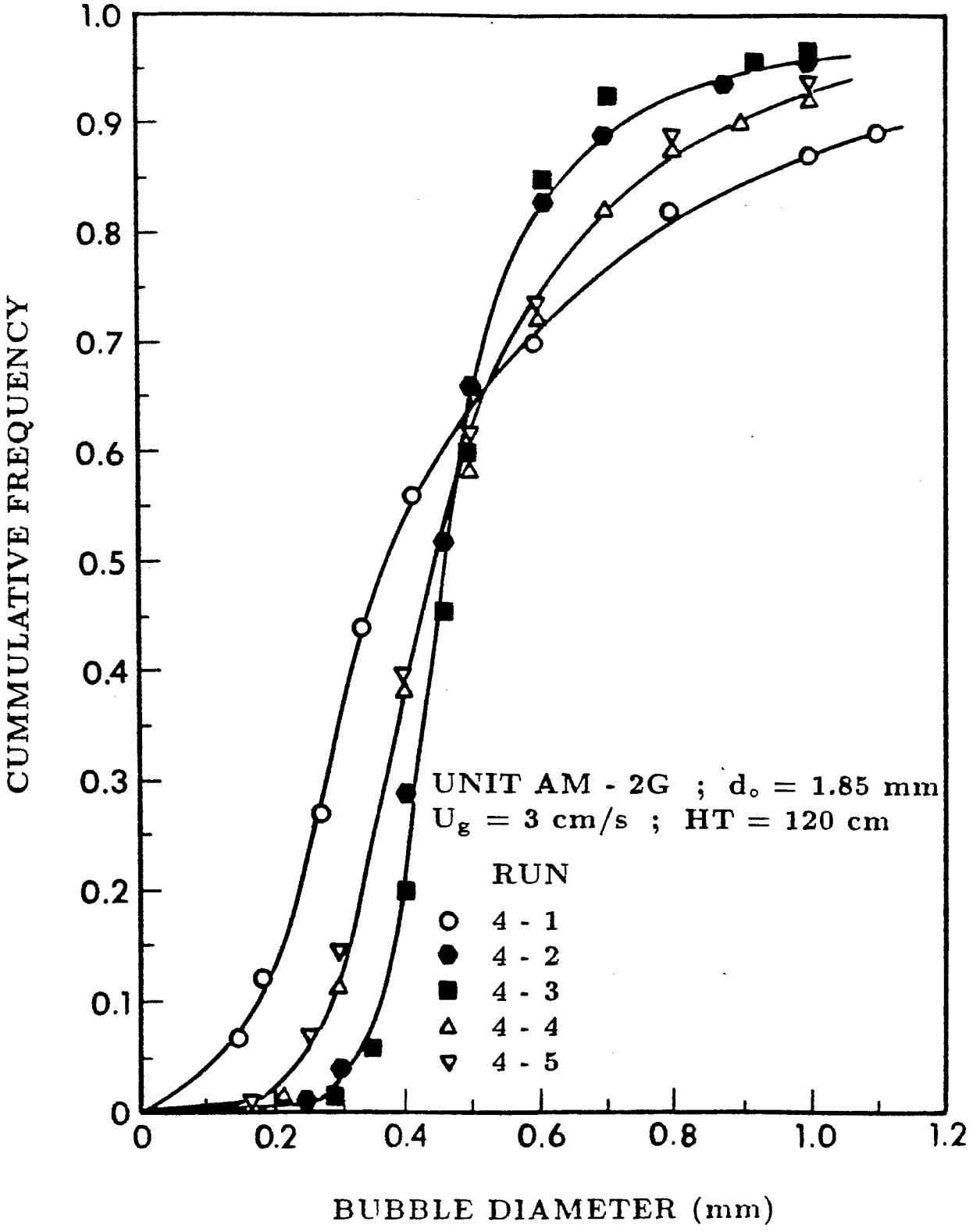

Figure 8. Effect of flow regime on the bubble size distribution (by photography; open symbols - "foamy" regime; solid symbols - "non-foamy" regime; ○ - T = 265 °C, FT-300; ● - T = 265 °C, FT-300; ■ - T = 200 °C, FT-300; △ - T = 265 °C, 5% stearyl alcohol (SA) + FT-300; ▽ - T = 265 °C, 5% SA + 5% stearic acid + FT-300)

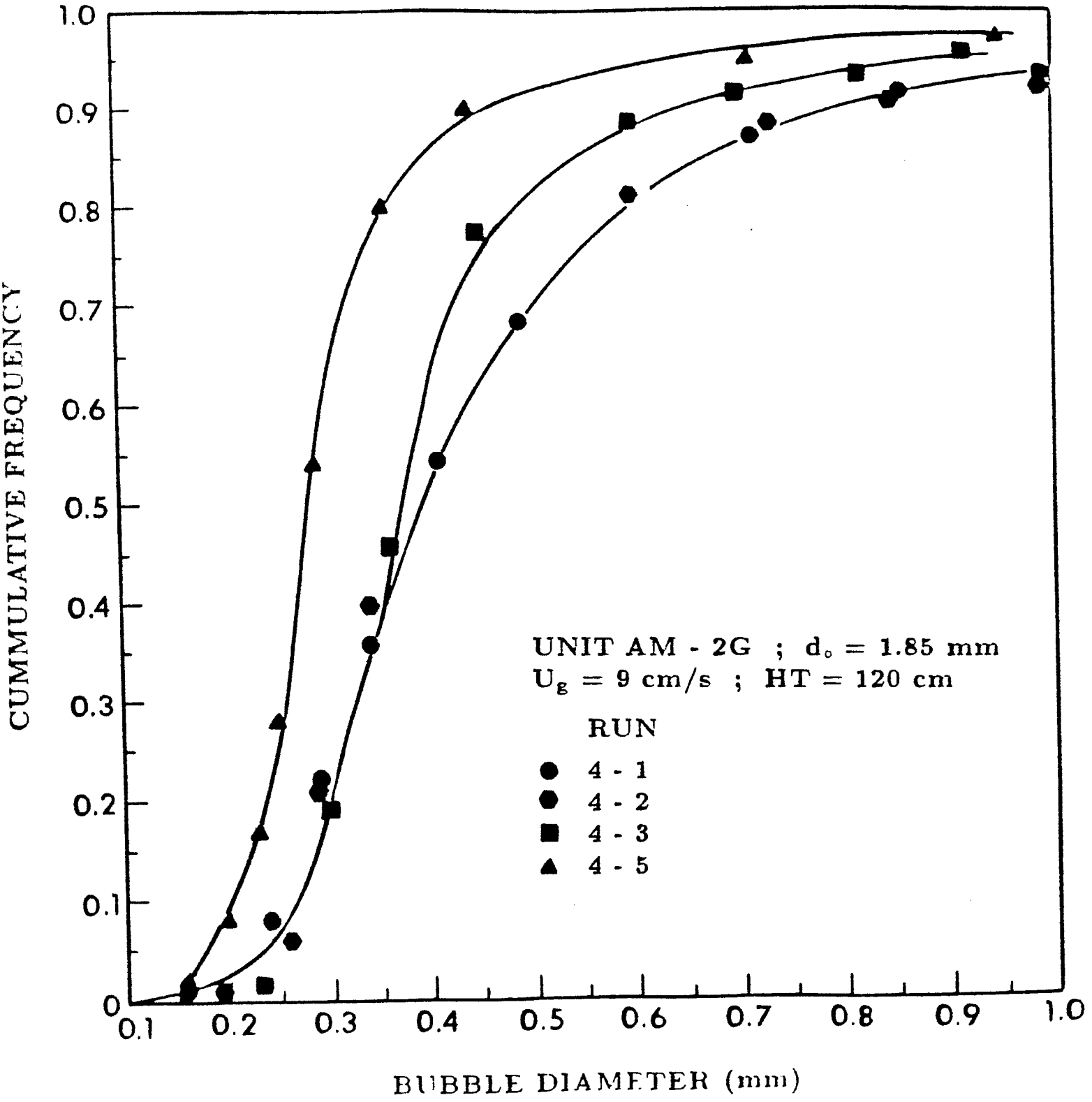

Figure 9. Effect of flow regime on the bubble size distribution (by photography; "non-foamy" regime; ● - T = 265 °C, FT-300; ⬢ - T = 265 °C, FT-300; ■ - T = 200 °C, FT-300; ▲ - T = 265 °C, 5% stearyl alcohol + 5% stearic acid + FT-300)

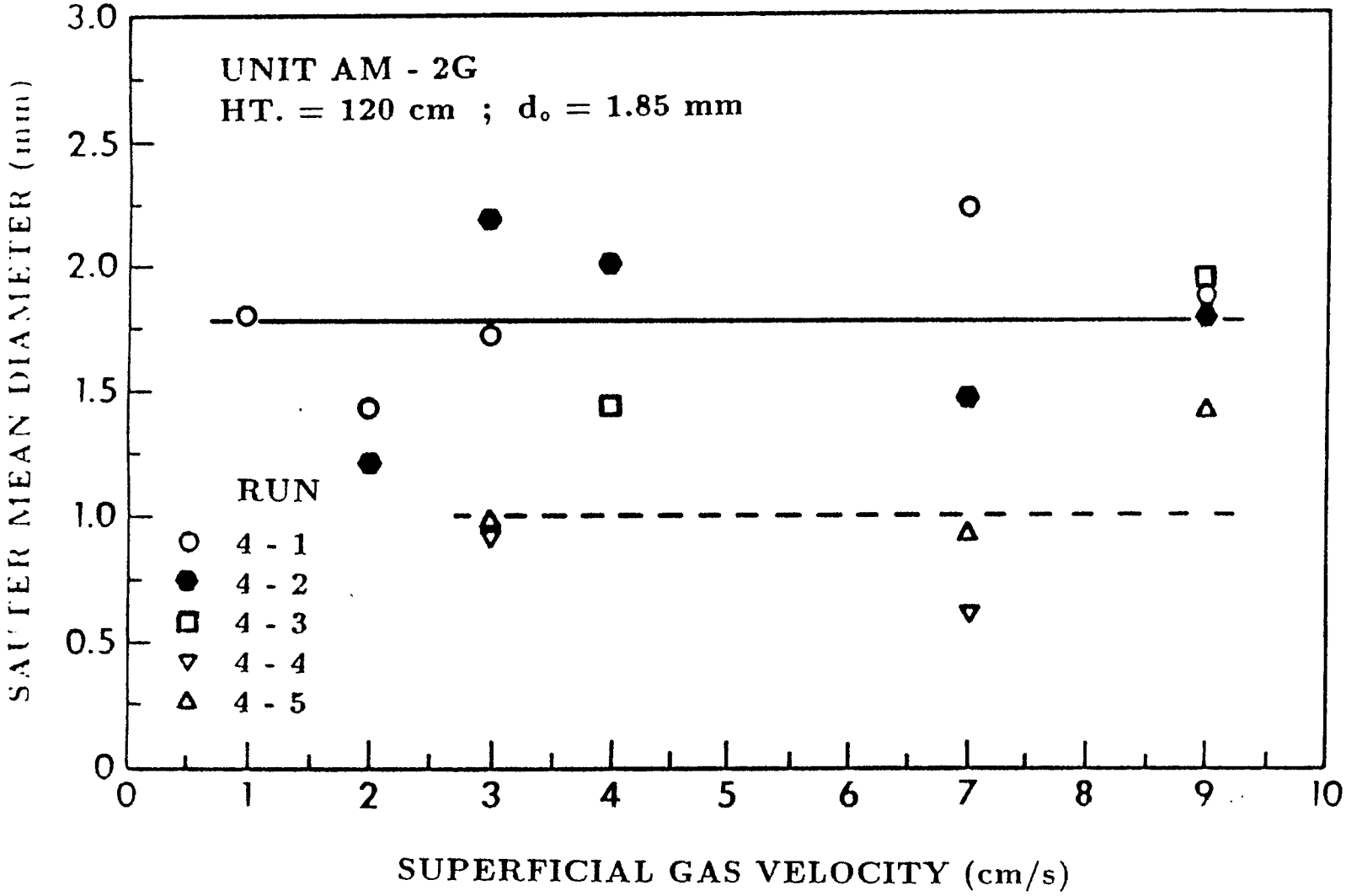

Figure 10. Effect of operating conditions on the Sauter mean diameter (by photography; open symbols - increasing gas velocities; solid symbols - decreasing gas velocities; ○ - T = 265 °C, FT-300; ● - T = 265 °C, FT-300; □ - T = 200 °C, FT-300; ▽ - T = 265 °C, 5% stearyl alcohol (SA) + FT-300; △ - T = 265 °C, 5% SA + 5% stearic acid + FT-300)

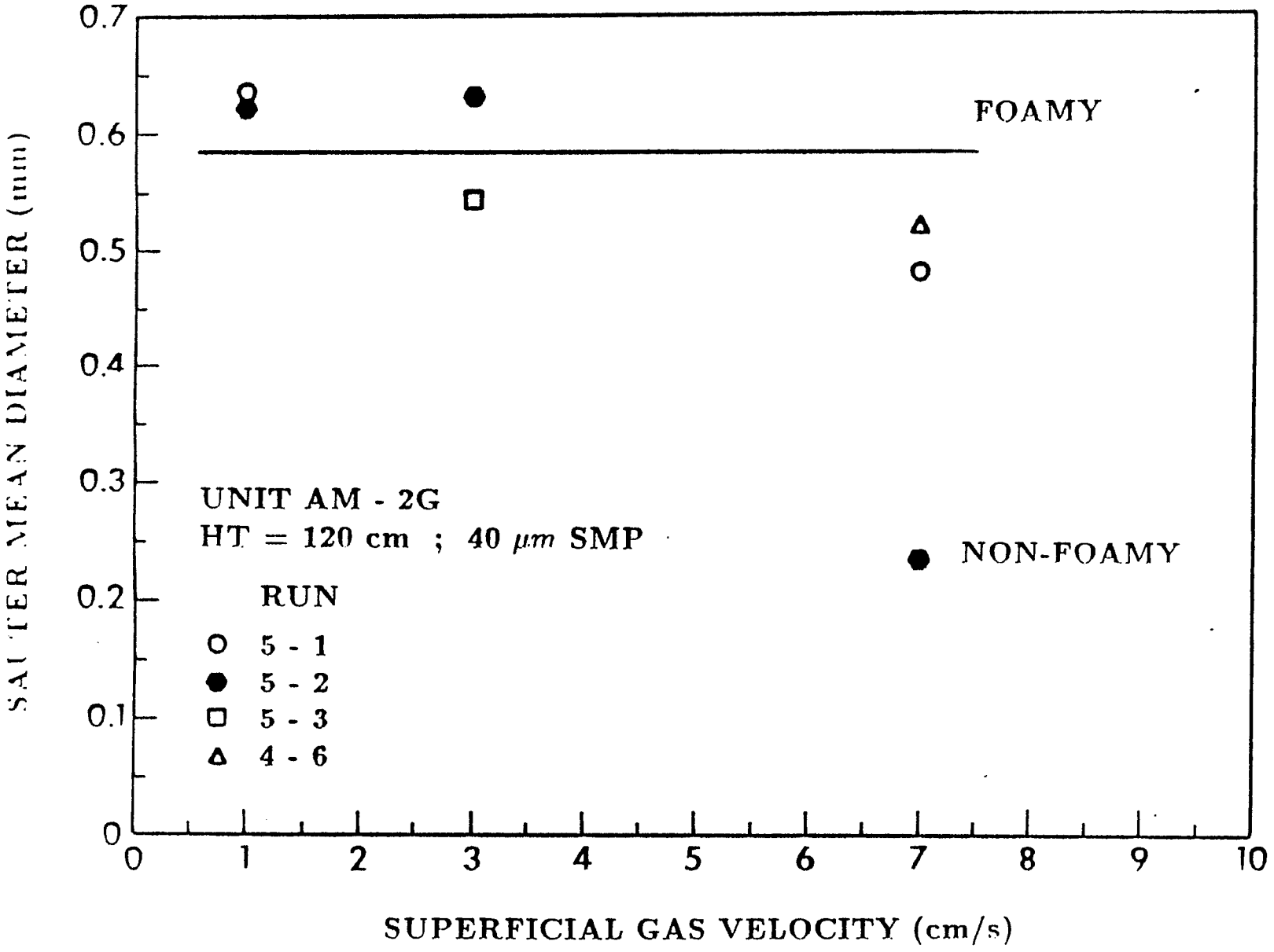

Figure 11. Effect of operating conditions on the Sauter mean diameter (by photography; open symbols - increasing gas velocities; solid symbols - decreasing gas velocities; ○ - T = 265 °C, FT-300; ● - T = 265 °C, FT-300; □ - T = 200 °C, FT-300; △ - T = 265 °C, 5% stearyl alcohol + 5% stearic acid + FT-300)

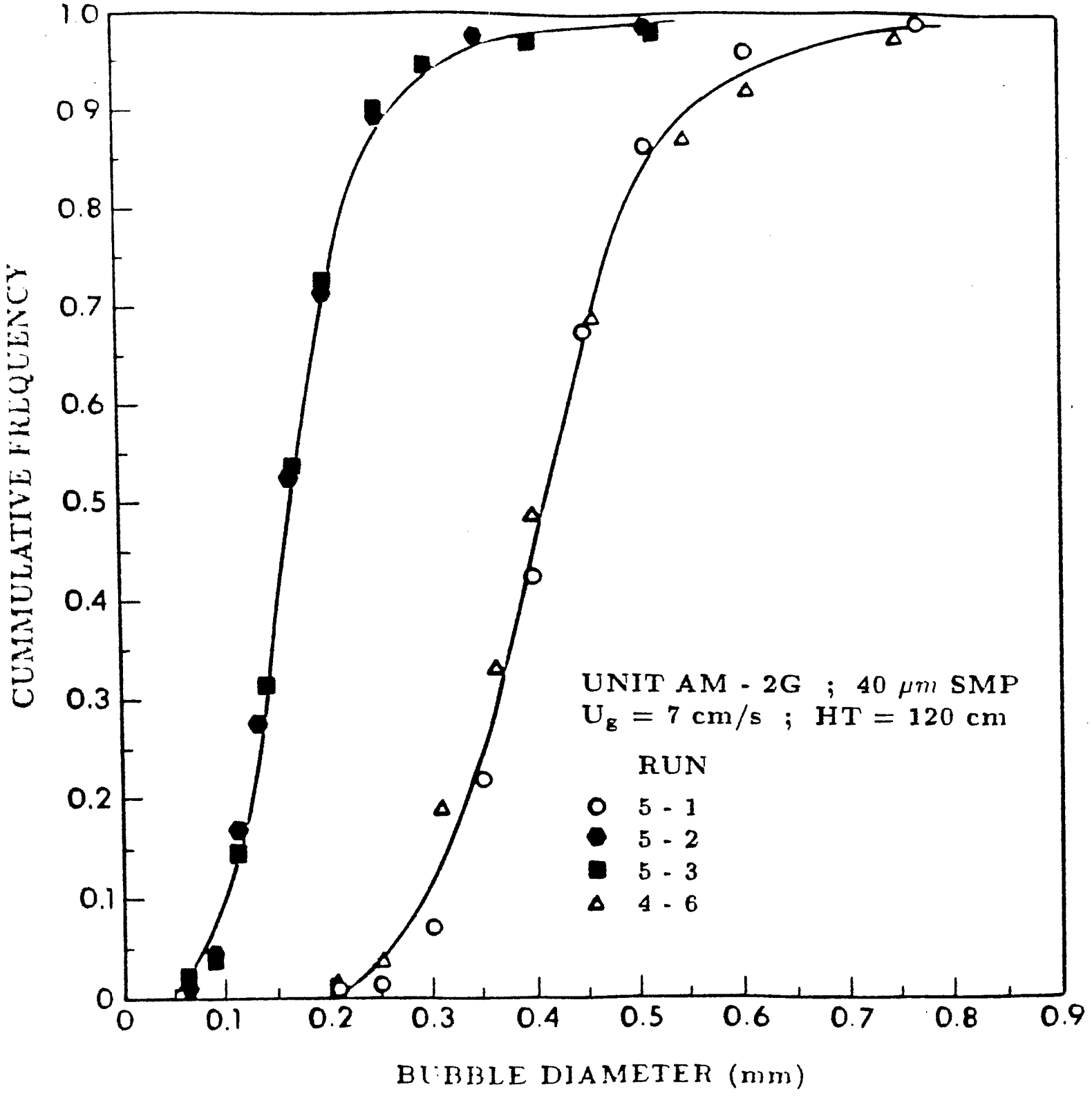

Figure 12. Effect of flow regime on the bubble size distribution (by photography; open symbols - "foamy" regime; solid symbols - "non-foamy" regime; ○ - T = 265 °C, FT-300; ● - T = 265 °C, FT-300; ■ - T = 200 °C, FT-300; △ - T = 265 °C, 5% stearyl alcohol + 5% stearic acid + FT-300)